Available online at www.sciencedirect.com

ScienceDirect

Mendeleev Commun., 2024, **34**, 725–728

Mendeleev Communications

Pt/C electrocatalysts based on N-doped carbon materials from waste plant biomass

Daria V. Chernysheva,*[a] Victor A. Klushin,[a] Anastasia A. Alekseenko,[b] Elizaveta A. Moguchikh,[b] Evgeny A. Kolesnikov,[c] Mikhail V. Gorshenkov,[c] Vasily V. Kaichev,[d] Lev N. Fesenko[a] and Nina V. Smirnova[a]

[a] *Research Institute of Nanotechnology and New Materials, Platov South-Russian State Polytechnic University, 346428 Novocherkassk, Russian Federation. E-mail: da.chernysheva@mail.ru*
[b] *Department of Chemistry, Southern Federal University, 344006 Rostov-on-Don, Russian Federation*
[c] *National University of Science and Technology 'MISiS', 119049 Moscow, Russian Federation*
[d] *G. K. Boreskov Institute of Catalysis, Siberian Branch of the Russian Academy of Sciences, 630090 Novosibirsk, Russian Federation*

DOI: 10.1016/j.mencom.2024.09.032

The N-doped carbon material obtained by thermochemical conversion of a polycondensation product of a liquid fraction of humins (a waste product of plant biomass conversion into furan derivatives) with the nitrogen-containing crosslinking component melamine was investigated as a support in Pt/C electrocatalysts for the oxygen reduction reaction.

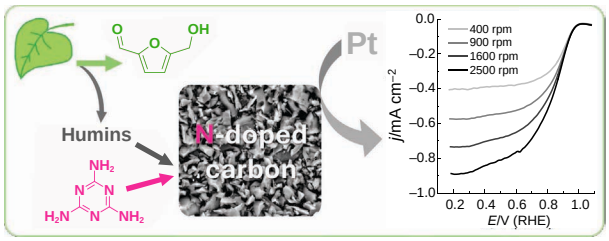

Keywords: nitrogen-doped carbon material, renewable plant biomass waste, humins, carbon support, electrocatalysts, oxygen reduction reaction.

Common catalysts for the oxygen reduction reaction (ORR) in low-temperature fuel cells are materials with nanosized platinum particles deposited on a carbon support.[1] The microstructure and composition of the carbon support significantly affect the properties of catalysts providing an accessible surface for the attachment of Pt nanoparticles, the necessary conductivity for electron transfer and transport of products and reagents.[2–4] To increase the catalytic activity of Pt/C, carbon materials (CMs) are modified with heteroatoms (N, S, P, *etc*.).[5–7] Surface defects arising from the embedding of heteroatoms act as active centers for the deposition of metal nanoparticles, providing uniformity of distribution and increasing affinity to the substrate, which leads to an increase in the catalytic activity and stability of Pt/C electrocatalysts.[8,9]

The direct doping method (*in situ*) consists in the synthesis of CMs with simultaneous uniform introduction of heteroatoms into the carbon framework.[10] The use of liquid wastes of chemical processing of plant biomass as a carbon source opens new opportunities for obtaining doped functional materials with controlled composition and surface architecture due to uniform doping in the liquid phase.[11] Such liquid wastes include humins (furan oligomers and polymers with a complex molecular structure) formed in the catalytic conversion of plant biomass into furan derivatives, so-called platform chemicals for the synthesis of practically valuable chemicals and materials.[12]

Depending on the conditions of carbohydrate processing, the yield of humins can reach 40%.[12,13] Therefore, the rational using of this waste requires the development of simple and efficient ways to convert humins into high value-added products. Previously, we used humins to create CMs for electrodes of double-layer supercapacitors.[11,14,15]

In this work, we investigated the possibility of using the N-doped carbon material from humins, waste of plant biomass processing, as a support for platinum nanoparticles in Pt/C electrocatalysts of the ORR.

The N-doped carbon material (NH-CK) was prepared by thermochemical conversion of a polycondensation product of a liquid fraction of humins (a waste product of 5-hydroxymethylfurfural synthesis) and the nitrogen-containing crosslinking component melamine in a weight ratio of 1 : 1. The components were thoroughly ground and incubated at 180 °C for 1 h in air environment to result in a solid brittle porous nitrogen-containing polymer (NH), which was sequentially carbonized and activated at 1000 °C using KOH in a horizontal tube furnace in a stream of N_2 according to a previously reported procedure.[11,14] In order to establish the influence of the doping heteroatom on the properties of the resulting carbon support in the Pt/C electrocatalyst, an undoped carbon material (H-CK) was prepared as described above; in this case the polymerization of humins was performed without the addition of crosslinking agents prior to thermochemical conversion.

The morphology and chemical composition of the resulting N-doped carbon material (NH-CK) was investigated by scanning electron microscopy (SEM) with energy dispersive X-ray microanalysis (EDX)† (Figure 1, Table 1).

According to the EDX data (Table 1), thermochemical conversion of the initial NH polymer significantly increased the carbon content. The amount of nitrogen decreased due to partial destruction of melamine with the formation of ammonia and CO_2 under the action of KOH and water in the process of thermochemical conversion. As found earlier,[11] under these conditions, nitrogen incorporated into the carbon framework

† A Quanta 200 scanning electron microscope combined with an EDAX Genesis XVS 30 X-ray microanalysis system.

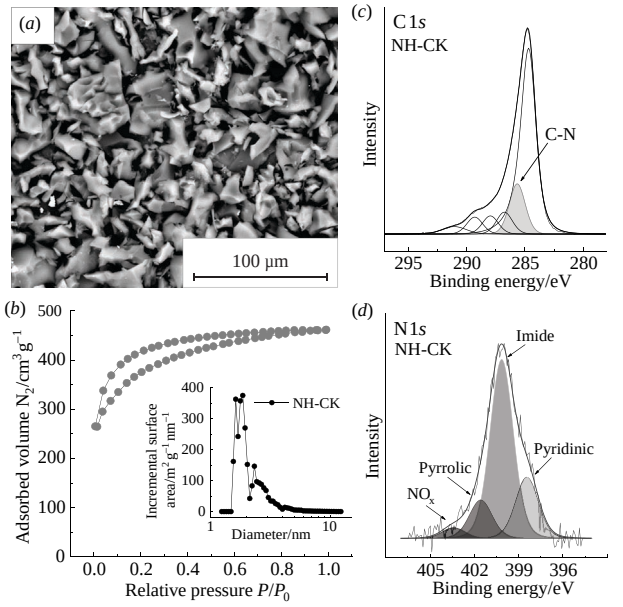

Figure 1 Structural properties of NH-CK: (*a*) SEM image, (*b*) adsorption–desorption isotherm (inset: BJH pore size distribution), and (*c*) C 1*s* and (*d*) N 1*s* core-level spectra.

through the formation of bonds with neighboring carbon atoms (Scheme S1, see Online Supplementary Materials). The presence of nitrogen in NH-CK was confirmed by XPS‡ [Figures 1(*c*),(*d*)]. According to published data,[16] the C 1*s* peaks at 284.8, 285.7, 286.7, 288.0, 289.3, and 290.8 eV can be attributed to carbon forming C=C (sp^2), C–N, C–O, C=O, and O–C=O bonds and π–π* excitation in graphite-like carbon, respectively. Deconvolution of the N 1*s* spectrum [Figure 1(*d*)] showed peaks at 398.5, 400.2, 401.6, and 403.4 eV related to pyridinic, imide, pyrrolic, and pyridine N-oxide surface functional groups, respectively.[16]

Trace amounts of Si were present in the CM as a result of chemical activation by alkali during calcination in a tubular furnace equipped with a ceramic tube. The presence of Na in humin-based polymers was explained by the method of 5-hydroxymethylfurfural synthesis.[11]

The porous structure of the carbon support is responsible for high catalytic activity of the Pt/C materials: it determines the rates of gas and ion mass transfer during the catalyst operation and the availability of Pt nanoparticles for reagents.[3] Figure 1(*b*) illustrates the specific surface area (SSA) and porosity§ of the NH-CK material. The nitrogen adsorption isotherm can be attributed to type I according to the IUPAC classification, which indicates the presence of micropores in the material. However, its hysteresis loop belongs to type H4, which is characteristic of a combination of both micropores and mesopores in the CM.[19] In addition, a wide pore size distribution obtained by the BJH method was observed due to a long hysteresis loop [inset in Figure 1(*b*)]. The SSA of chemically activated NH-CK calculated by the BET method was 1309 m^2 g^{-1} (Table 1).

Table 1 Elemental composition (according to EDX data), values of SSA, pore volume, and pore size of the NH-CK carbon material.

Material	Atomic content (EDX) (at%)					SSA_{BET}/ m^2 g^{-1}	Pore volume[a]/ cm^3 g^{-1}	Pore size/ nm
	C	O	N	Na	Si			
NH	37.9	8.5	53.3	0.3	–	–	–	–
NH-CK	85.4	10.5	4.0	–	0.1	1309	0.615	0.92

[a] Calculated by t-plot micropore volume.

The Pt/C catalysts were synthesized in a liquid phase with formaldehyde as a reducing agent[20] (for details, see Online Supplementary Materials). This method of depositing platinum nanoparticles is based on their growth directly on the surface of a carbon support, and heteroatoms embedded in the carbon framework can act as active crystallization centers and contribute to a more reliable fixation of associated metal particles. The mass loading of platinum in the electrocatalyst was determined by thermogravimetry after heating up to 800 °C. The platinum loading in the obtained Pt/NH-CK was close to the calculated one (23%), while the platinum loading in Pt/H-CK based on undoped CM was only 15%. It is well known that the deposition of Pt on the support is significantly influenced by the available surface area of the CM, the presence of mesopores and active sites for heterophase nucleation and growth of metal nanoparticles, and heteroatoms embedded in the carbon framework.[8] The platinum content of the catalyst based on the N-doped CM fully corresponds to the theoretically calculated value; unlike to catalysts based on the undoped CM, this can indicate a positive effect of embedded nitrogen on the adhesion strength of Pt nanoparticles and their resistance to mechanical detachment at the stage of filtering and washing of the catalyst during preparation.

The X-ray diffraction pattern¶ of the Pt/NH-CK sample has a typical appearance for similar materials [Figure 2(*a*)]. The average size of platinum crystallites calculated using the Scherrer equation was 3 nm, which slightly exceeds the value obtained based on the transmission electron microscopy analysis†† [Figure 2(*b*)].

Figure 3 shows the electrochemical properties of the Pt/NH-CK and Pt/H-CK materials in a three-electrode cell.‡‡ Since

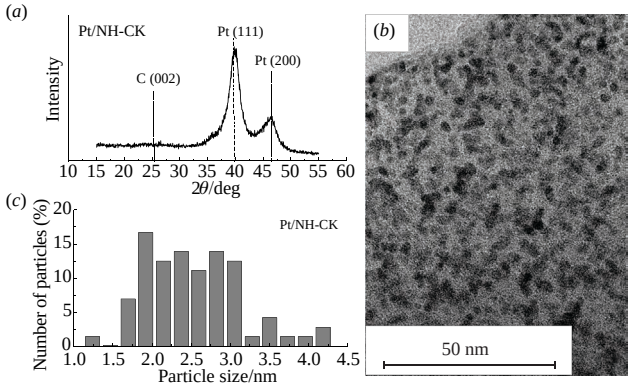

Figure 2 (*a*) X-ray diffraction pattern, (*b*) TEM image, and (*c*) size distribution of platinum nanoparticles of the Pt/NH-CK catalyst.

‡ The XPS measurements were performed on an X-ray photoelectron spectrometer equipped with a PHOIBOS-150-MCD-9 hemispherical analyzer and an XR-50 X-ray radiation source (SPECS Surface Nano Analysis GmbH, Germany). The core-level spectra were recorded using Al Kα radiation ($h\nu$ = 1486.6 eV). The charge correction was performed by setting the most intense C 1*s* peak at 284.8 eV.

§ The SSA values of CMs were determined using a NOVA 1200e surface area and porosity analyzer (Quantachrome, the United States) and calculated from nitrogen adsorption/desorption isotherms according to the Brunauer–Emmett–Teller (BET) method. The CM sample was degassed at 150 °C in a vacuum for 24 h before N_2 adsorption measurements carried out at 77 K. The pore size distribution was calculated from desorption branches of isotherms using the Barrett–Joyner–Halenda (BJH) method.[17] The t-method was used to determine the volume of micropores in the presence of mesopores.[18]

¶ XRD analysis was performed on an ARL X'TRA powder diffractometer using Cu Kα radiation.[20]

†† The TEM measurements were made on a JEM-2100 microscope (JEOL, Japan) at an accelerating voltage of 200 kV.

‡‡ The working electrode was a catalytic layer based on catalytic 'ink' formed on a glassy carbon disk electrode.[21] The reference electrode was saturated Ag/AgCl, and the counter electrode was Pt wire. All potentials are given relative to a reversible hydrogen electrode (RHE). The measurements were carried out using a Pine Research MSR Rotator (the United States).

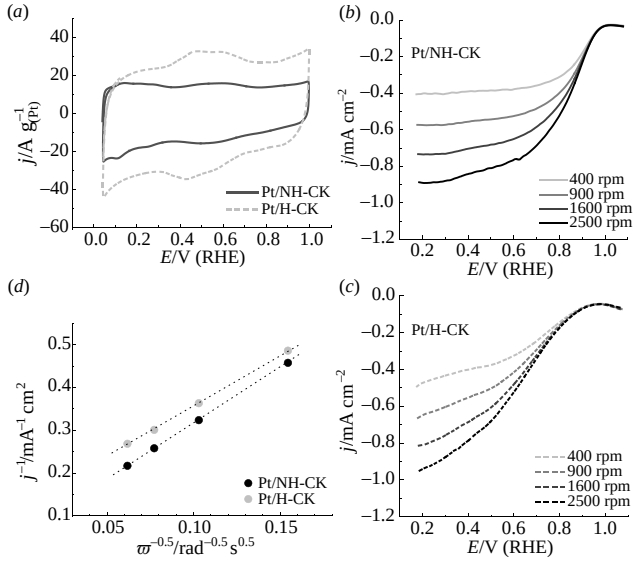

Figure 3 Electrochemical properties of the Pt/NH-CK (solid lines) and Pt/H-CK (dashed lines) catalysts after the standardization stage: (*a*) CV curves (0.1 M $HClO_4$ saturated with Ar; 20 mV s^{-1}); (*b*),(*c*) LSV curves of ORRs at RDE speeds of 400, 900, 1600, and 2500 rpm (0.1 M $HClO_4$ saturated with O_2; 20 mV s^{-1}); and (*d*) j^{-1}–$\omega^{-0.5}$ relationship at a potential of 0.5 V (RHE).

alkali activation promoted the formation of the developed SSA (Table 1), this was reflected in the shapes of the CV curves of both electrocatalysts, namely, the expansion of the double-layer region [Figure 3(*a*)]. The pseudo-capacitance peaks at 0.4–0.7 V (RHE) observed in the CV curves were related to the conversion of quinone–hydroquinone groups on the carbon surface.[22]

In a potential range of 0.04–0.30 V (RHE) [Figure 3(*a*)], peaks of hydrogen adsorption and desorption in the CV curve indicated that the amount of electricity spent for hydrogen adsorption exceeded that for desorption due to the ongoing process of hydrogen spillover.[23] The electrochemically active surface areas (ESAs) of the Pt/NH-CK and Pt/H-CK catalysts were 18 ± 2 m^2 $g_{(Pt)}^{-1}$ (for details, see Online Supplementary Materials).

The study of the reaction kinetics of oxygen electroreduction in acidic medium by the Koutecký–Levich method[20,24] (Online Supplementary Materials) showed that it proceeded mainly by a four-electron mechanism. The slightly prominent reduction wave at 0.3 V in the LSV curves of the Pt/NH-CK catalyst [Figure 3(*b*)] can be related to two-electron reduction of oxygen on the active sites of the nitrogen-doped carbon support.[25] However, note that, during the operation of low-temperature fuel cells, the voltage is much higher than 0.3 V; therefore, the two-electron ORR did not take place at the cathode. Possible ORR mechanisms are provided in Online Supplementary Materials.

The kinetic current densities (j_k) at a potential of 0.5 V selected in the range of the limiting diffusion current were 17.4 and 8.2 mA cm^{-2} for Pt/NH-CK and Pt/H-CK, respectively (see Online Supplementary Materials). In addition, the Pt/NH-CK catalyst exhibited excellent stability during stress testing (Figure S1). Thus, the ESA decreased by only 4.7% after multiple voltammetric cyclic potential changes at a rate of 100 mV s^{-1} for 3000 cycles in a potential range of 0.6–1.0 V (RHE) in the air-saturated electrolyte.

Thus, the N-doped carbon material was prepared by thermochemical conversion of a polycondensation product of liquid wastes from chemical processing of plant biomass into furan derivatives and the nitrogen-containing crosslinking component melamine. The composition and microstructure of the N-doped CM were determined by physicochemical methods. For the first time, the use of this carbon material as a support in Pt/C electrocatalysts was investigated. The Pt/NH-CK electrocatalyst based on the nitrogen-doped carbon material exhibited greater electrocatalytic activity in the oxygen reduction reaction than that of a catalyst with the undoped carbon support (Pt/H-CK).

Studies were supported by the Russian Science Foundation (project no. 23-23-00399). The authors are grateful to the Shared Research Center ‘Nanotechnologies’ of Platov South-Russian State Polytechnic University.

Online Supplementary Materials

Supplementary data associated with this article can be found in the online version: 10.1016/j.mencom.2024.09.032.

References

1 X. Hu, B. Yang, S. Ke, Y. Liu, M. Fang, Z. Huang and X. Min, *Energy Fuels*, 2023, **37**, 11532; https://doi.org/10.1021/acs.energyfuels.3c01265.
2 W. Mabhulusa, K. E. Sekhosana and X. Fuku, *Int. J. Electrochem. Sci.*, 2024, **19**, 100524; https://doi.org/10.1016/j.ijoes.2024.100524.
3 I. C. Gerber and P. Serp, *Chem. Rev.*, 2020, **120**, 1250; https://doi.org/10.1021/acs.chemrev.9b00209.
4 C. Durante, *Curr. Opin. Electrochem.*, 2022, **36**, 101119; https://doi.org/10.1016/j.coelec.2022.101119.
5 T. Asefa and X. Huang, *Chem. – Eur. J.*, 2017, **23**, 10703; https://doi.org/10.1002/chem.201700439.
6 Z. Ma, Z. P. Cano, A. Yu, Z. Chen, G. Jiang, X. Fu, L. Yang, T. Wu, Z. Bai and J. Lu, *Angew. Chem., Int. Ed.*, 2020, **59**, 18334; https://doi.org/10.1002/anie.202003654.
7 V. K. Kochergin, R. A. Manzhos, I. I. Khodos and A. G. Krivenko, *Mendeleev Commun.*, 2022, **32**, 492; https://doi.org/10.1016/j.mencom.2022.07.020.
8 A. S. Pushkarev, I. V. Pushkareva, M. V. Kozlova, M. A. Solovyev, S. I. Butrim, J. Ge, W. Xing and V. N. Fateev, *Russ. J. Electrochem.*, 2022, **58**, 529; https://doi.org/10.1134/S1023193522070114.
9 J. Martin, J. Melke, C. Njel, A. Schökel, J. Büttner and A. Fischer, *ChemElectroChem*, 2021, **8**, 4835; https://doi.org/10.1002/celc.202101162.
10 Y. Gao, Q. Wang, G. Ji, A. Li and J. Niu, *RSC Adv.*, 2021, **11**, 5361; https://doi.org/10.1039/d0ra08993a.
11 D. V. Chernysheva, E. A. Sidash, M. S. Konstantinov, V. A. Klushin, D. V. Tokarev, V. E. Andreeva, E. A. Kolesnikov, V. V. Kaichev, N. V. Smirnova and V. P. Ananikov, *ChemSusChem*, 2023, **16**, e202202065; https://doi.org/ 10.1002/cssc.202202065.
12 V. P. Kashparova, D. V. Chernysheva, V. A. Klushin, V. E. Andreeva, O. A. Kravchenko and N. V. Smirnova, *Russ. Chem. Rev.*, 2021, **90**, 750; https://doi.org/10.1070/RCR5018.
13 S. Liu, Y. Zhu, Y. Liao, H. Wang, Q. Liu, L. Ma and C. Wang, *Appl. Energy Combust. Sci.*, 2022, **10**, 100062; https://doi.org/10.1016/j.jaecs.2022.100062.
14 D. V. Chernysheva, Y. A. Chus, V. A. Klushin, T. A. Lastovina, L. S. Pudova, N. V. Smirnova, O. A. Kravchenko, V. M. Chernyshev and V. P. Ananikov, *ChemSusChem*, 2018, **11**, 3599; https://doi.org/10.1002/cssc.201801757.
15 D. V. Chernysheva, N. V. Smirnova and V. P. Ananikov, *ChemSusChem*, 2024, **17**, e202301367; https://doi.org/10.1002/cssc.202301367.
16 D. Chernysheva, M. Konstantinov, E. Sidash, T. Baranova, V. Klushin, D. Tokarev, V. Andreeva, E. Kolesnikov, V. Kaichev, M. Gorshenkov and N. Smirnova, *Symmetry*, 2023, **15**, 846; https://doi.org/10.3390/sym15040846.
17 M. Thommes, K. Kaneko, A. V. Neimark, J. P. Olivier, F. Rodriguez-Reinoso, J. Rouquerol and K. S. W. Sing, *Pure Appl. Chem.*, 2015, **87**, 1051; https://doi.org/10.1515/pac-2014-1117.
18 A. Galarneau, F. Villemot, J. Rodriguez, F. Fajula and B. Coasne, *Langmuir*, 2014, **30**, 13266; https://doi.org/10.1021/la5026679.
19 L. Hou, L. Lian, D. Li, G. Pang, J. Li, X. Zhang, S. Xiong and C. Yuan, *Carbon*, 2013, **64**, 141; https://doi.org/10.1016/j.carbon.2013.07.045.
20 K. O. Paperzh, A. A. Alekseenko, V. A. Volochaev, I. V. Pankov, O. A. Safronenko and V. E. Guterman, *Beilstein J. Nanotechnol.*, 2021, **12**, 593; https://doi.org/ 10.3762/bjnano.12.49.
21 K. Paperzh, A. Alekseenko, O. Safronenko, A. Nikulin, I. Pankov and V. Guterman, *Colloid Interface Sci. Commun.*, 2021, **45**, 100517; https://doi.org/10.1016/j.colcom.2021.100517.

22 G.-F. Han, F. Li, W. Zou, M. Karamad, J.-P. Jeon, S.-W. Kim, S.-J. Kim, Y. Bu, Z. Fu, Y. Lu, S. Siahrostami and J.-B. Baek, *Nat. Commun.*, 2020, **11**, 2209; https://doi.org/10.1038/s41467-020-15782-z.

23 R. Bhowmick, S. Rajasekaran, D. Friebel, C. Beasley, L. Jiao, H. Ogasawara, H. Dai, B. Clemens and A. Nilsson, *J. Am. Chem. Soc.*, 2011, **133**, 5580; https://doi.org/0.1021/ja200403m.

24 K. Shinozaki, J. W. Zack, R. M. Richards, B. S. Pivovar and S. S. Kocha, *J. Electrochem. Soc.*, 2015, **162**, F1144; https://doi.org/10.1149/2.1071509jes.

25 J. An, Y. Feng, Q. Zhao, X. Wang, J. Liu and N. Li, *Environ. Sci. Ecotechnol.*, 2022, **11**, 100170; https://doi.org/10.1016/j.ese.2022.100170.

Received: 8th April 2024; Com. 24/7450